*Resolving the Rise and Fall of Star Formation in Galaxies*
*Proceedings IAU Symposium No. 373, 2023*
*T. Wong & W.-T. Kim, eds.*
doi:10.1017/S1743921322004902

# Milky Way: structure via live potentials

**Eva Durán-Camacho and Ana Duarte-Cabral**

School of Physics and Astronomy, Cardiff University, Queens Buildings, The Parade, Cardiff CF24 3AA, UK
email: durancamachoe@cardiff.ac.uk

**Abstract.** We use the AREPO numerical code to model the structure of a Milky Way like galaxy (MW) via a suite of simulations composed of a stellar disc and bulge, a dark matter halo, and a gaseous disc under isothermal conditions. For each model, we produce longitude velocity ($l$-$v$) maps of the gas surface densities to extract the skeletons of the main features (arms, bar), and the contours defining the terminal velocities of the gas. We compare these with observations via a number of diagnostic tools, and select the model that best reproduces the main observed features of the Milky Way.

**Keywords.** Galaxy: structure, Galaxy: kinematics and dynamics, galaxies: spiral

## 1. Introduction

In order to understand the specific role that the large-scale galactic features (spiral arms/bar) have on star formation within the Milky Way, we first need to pin down its anatomy. However, the structure of the Milky Way has been a subject of study for decades and there is still no real consensus on its exact morphology, mostly due to observational limitations (e.g. Elmegreen 1985). Nevertheless, our Galaxy is unanimously believed to be spiral (e.g. Xu et al. 2016) and host a Galactic bar (e.g. Weinberg 1992).

Aiming to model the spiral/bar pattern of the Milky Way using numerical simulations, the most common approach is to set up an analytical gravitational potential that mimics the external potential from the stars and dark matter halo (e.g. Dobbs et al. 2013; Smith et al. 2020). Another approach is to use stellar and dark matter particles to recreate the galactic structure self-consistently through the N-body dynamical evolution of the system (i.e. the so-called "live potentials"). However, most models that focus on the Milky Way typically set out to produce a MW-type galaxy, rather than effectively attempting to fit the observed structure. One exception are the works of Pettit et al. (2014, 2015) who produce $l$-$v$ maps from their models and compare them to observations via $\chi^2$ statistics. Their models with live potentials are able reproduce the observed spiral arm features, but fail to generate an inner bar. The ability to reproduce the anatomy of the MW in simulations is essential to study the role of the Galactic structure on star formation, but the choice of live-versus-fixed potentials can have a strong impact on the conclusions, as it changes the gas response to the potential. In this context, our aim is to reproduce the Mily Way structure using the self-consistent evolution of live-potentials.

## 2. Overview

Our simulations are performed with the moving-mesh code AREPO (Springel 2010). Our primary goal is to re-create the overall structure of the MW (i.e. spiral pattern and central bar) through the N-body dynamical interaction of the stars over several Gyrs.

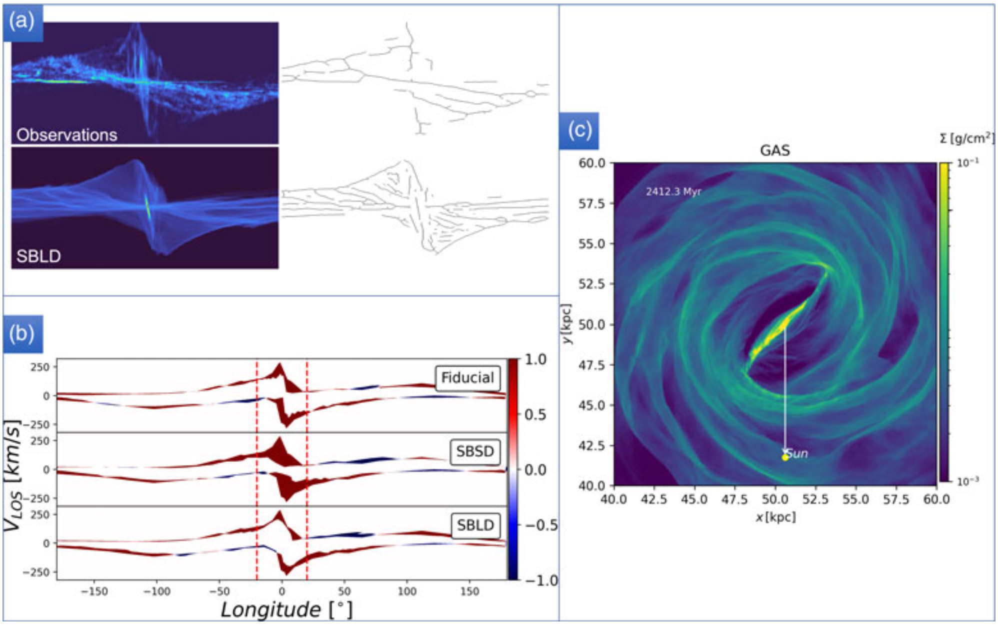


**Figure 1.** A) Left: $l$-$v$ maps of the observations (top) and the best model at its optimal time/viewing angle. Right: the respective extracted skeletons. The ranges of these $l$-$v$ are: $|V_{LOS}| \pm 280$ km/s and $|l| \pm 60°$. B) Terminal velocity comparison of the Dame et al. (2001) CO observations with our three different models (as labelled). Vertical dashed red lines delimit the inner and outer Galaxy regions ($|\,l\,| < 20°$). Red regions denote areas covered by the observations and not the models, and blue regions the reverse. C) Top-down view of the surface density of the gas of our best fit model (SBLD at a time $\sim 2.4$ Gyrs) with the Sun at 270°.

Therefore, we minimise the computational time spent on the hydrodynamical part of the code by having a relatively low resolution for the gas and isothermal equations of state.

The initial conditions for our MW models were setup using the moment-based code MAKENEWDISK, described in (Springel 2005). They consist of a dark matter halo, a rotationally supported disc of gas and stars, and a central stellar bulge. The dark matter halo and the stellar bulge follow an Hernquist density profile (Hernquist 1990), and the stellar disc follows an exponential surface density profile. We produce three different set ups for the stellar distribution: a Fiducial model based on the best fit model by Pettit et al. (2015); a model with a smaller bulge, and small disc (SBSD); and a model with a small bulge, and larger disc (SBLD). We also explore two different profiles for the gas distribution: same exponential surface density profile as the stars (i.e. the default of MAKENEWDISK); and a uniform surface density profile, as suggested by some observations (e.g. Ferriere et al. 2007). Full details on the parameters of these models can be found in Durán-Camacho et al. (in prep.).

To compare the structures produced by our six models to the observations, we produce $lv$-maps for each model, by looking at 20 snapshots from $1.4 - 2.9$ Gyrs through 24 different viewing angles each. We then find the best model with various different tests.

## 3. Results and discussion

To evaluate how our models perform at reproducing the morphology of the MW, we extract the spines that trace the main features in $lv$-space (i.e. the "skeletons") of the $^{12}$CO emission from Dame et al. (2001), and of our simulations (Fig. 1, panel A). We then use a statistical tool, the Symmetrized Modified Hausdorff Distance (SMHD,

https://doi.org/10.1017/S1743921322004902 Published online by Cambridge University Press

(Sormani et al. 2015), to compare the observed and modelled skeletons. We start by investigating the time evolution of the SMHD metric and select the snapshot at which the global SMHD metric was lowest for each model. We then investigate how the SMHD varies within that snapshot as a function of the observer's viewing angle, to select the optimal reproduction of the MW for each model. The best model overall is selected by comparing the SMHD metric values between models, as well as the terminal velocities reproduced by the models versus the observed ones (Fig. 1, panel B).

This analysis indicates that all models are similar at mimicking the outer Galaxy, but there is a clear difference between models in the inner Galaxy, showing SBSD as the least favourable model, and SBLD as the better one. This is mostly due to the larger velocity ranges it attains in the inner galaxy, and the better match of the skeleton structures towards the central part, with the formation of a bar that resembles that of the MW (with a bar pattern speed of $22\,\mathrm{km\,s^{-1}\,kpc^{-1}}$, and a length of $\sim 6\,\mathrm{kpc}$).

Finally, we analyse which gas profile best reproduces our MW, by creating 1D plots of the column density versus longitude. The equivalent distribution for the observations was obtained from the SED fitting of the dust continuum emission from $60 - 850\mu$m from IRAS and Planck (Wheelock et al. 1994, Collaboration 2016). We find that a uniform gas surface density distribution is a better (albeit not perfect) match to observations.

Overall, we find that the SBLD model with a uniform gas profile, at a time 2.4 Gyrs is our best fit (Fig. 1, panel C). We will use this model as the base configuration for more sophisticated modelling of the ISM in the MW.

## Supplementary material

To view supplementary material for this article, please visit https://doi.org/10.1017/S1743921322004902.

## References

Elmegreen, D. M. 1985, In Symposium-International Astronomical Union (Vol. 106, pp. 255–272). Cambridge University Press.

Xu, Y., Reid, M., Dame, T., Menten, K., Sakai, N., Li, J., Zheng, X. 2016, *Science Advances* 2(9), e1600878

Weinberg, M. D. 1992, *ApJ* 384, 81–94

Dobbs, C. L., Pringle, J. E. 2013, *MNRAS* 432(1), 653–667

Smith, R. J., Treß, R. G., Sormani, M. C., Glover, S. C., Klessen, R. S., Clark, P. C., Zucker, C. 2020, *MNRAS* 492(2), 1594–1613

Pettitt, A. R., Dobbs, C. L., Acreman, D. M., Price, D. J. 2014, *MNRAS* 444(1), 919–941

Pettitt, A. R., Dobbs, C. L., Acreman, D. M., Bate, M. R. 2015, *MNRAS* 449(4), 3911–3926

Springel, V. 2010, *MNRAS* 401(2), 791–851

Springel, V., Di Matteo, T., Hernquist, L. 2005, *MNRAS* 361(3), 776–794

Hernquist, L. 1990, *ApJ* 356, 359–364

Ferriere, K., Gillard, W., Jean, P. 2007, *ARAA* 467(2), 611–627

Dame, T. M., Hartmann, D., Thaddeus, P. 2001, *ApJ* 547(2), 792

Sormani, M. C., Magorrian, J. 2015, *MNRAS* 446(4), 4186–4204

Wheelock, S. L., Gautier, T. N., Chillemi, J., Kester, D., McCallon, H., Oken, C., ... Good, J. 1994, (No. NAS 1.26: 197335)

Collaboration, P., Ade, P. A. R., Aghanim, N., Akrami, Y., Aluri, P. K., Arnaud, M., ... Mennella, A. 2016